J Mater Sci
DOI 10.1007/s10853-015-9621-9

Hybrid metallic composite materials fabricated by sheathed powder compaction

Thaneshan Sapanathan[1,5] · Shahin Khoddam[2] · Saden H. Zahiri[3] · Abbas Zarei-Hanzaki[4] · Raafat Ibrahim[1]

Received: 4 August 2015 / Accepted: 25 November 2015

Abstract A new process, sheathed powder compaction (SPC), was proposed to fabricate hybrid metallic composite samples at room temperature. The process involves densification of fine powder in an annulus sheath under combined moderate pressure and shear. Hybrid samples of copper annular with aluminum powder were produced to demonstrate the merits of the process. The fabricated samples were characterized and explored using electron microscopy, micro hardness, micro shear punch tests and density ratio measurements. Comparing "shear punch response" of the samples in the Al region with those of commercially pure aluminum and Al 5005-H34 samples showed an excellent shearing strength in the region. The electron backscatter diffraction analyses and scanning electron microscopy observations suggested that the substantially enhanced strength was facilitated by a significant SPC induced grain refinement. Moreover, the annular sheath (copper) also showed significant grain refinement due to the process. These demonstrated promising potentials of the SPC to manufacture hybrid metals with concurrent grain refinement at room temperature under moderate processing conditions.

Graphical Abstract

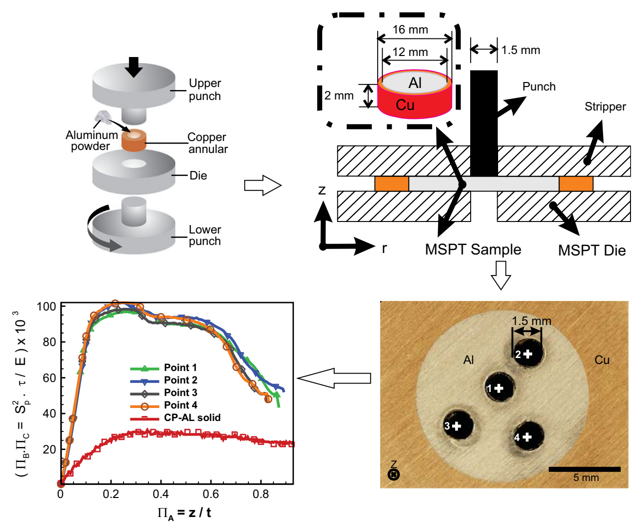

✉ Shahin Khoddam
shahin@deakin.edu.au

[1] Department of Mechanical & Aerospace Engineering, Monash University, Clayton, VIC 3800, Australia

[2] Institute for Frontier Materials, Deakin University, GTP Building, 75 Pigdons Road, Waurn Ponds, VIC 3216, Australia

[3] CSIRO Materials Science and Engineering (CMSE), Clayton, VIC 3169, Australia

[4] Department of Materials Engineering, Tehran University, Tehran, Iran

[5] Laboratoire Roberval, UMR CNRS 7337, Université de Technologie de Compiègne, 60203 Compiègne, France

Introduction

Metal composites are attractive solutions to design modern engineering materials based on the choice of materials, shape and length scale [1, 2]. "Architectured materials", a sub-class of metal composites, have been introduced to serve the increasing demand of advanced materials [3, 4]. Architectural features as well as multifunctional and structural properties of these materials are governed by their inner architecture of the metallic elements. These materials provide various functional properties such as thermal insulation, magnetic properties, acoustic damping, and energy absorption with enhanced mechanical properties such as weight reduction and strength improvement [5]. Incorporating innovative severe plastic deformation processes (ISPD) (e.g., [6, 7]) in the fabrication of metal composites, enhances their properties [3]. The synergetic effect of high pressure and shear has been recently utilized in a number of SPD-based techniques to fabricate the copper clad aluminum composites at warm/room temperatures (e.g., fabricating bimetallic copper–aluminum tube [8], cold welding using ECAP [9] and axi-symmetric forward spiral composite extrusion process [10, 11]).

The conventional high pressure torsion (HPT) process is also a popular technique to produce bulk, powders, intermetallic, and ceramics [12] materials with significant grain refinement and excellent mechanical properties. Ultra fine grained materials are particularly attractive in the applications of miniaturized parts such as components in biomedical devices, microelectromechanical systems (MEMS) [13], small diameter teeth implants, micro springs [14], and microsystems [15]. However, the conventional HPT processing of powder materials requires high process conditions (e.g., 2.5–15 GPa with 5–60 rotations) for successful consolidation of the particles [16–21]. Therefore, it is desirable to find methods to reduce the required conditions.

The development of architectured materials with concurrent grain refinement often requires new processing methods (e.g., [22, 23]). A new and simple process, sheathed powder compaction (SPC) is proposed here, to produce hybrid metallic composite disks. The technique may be classified as confined high pressure torsion (CHPT) processing of the annular sheath filled with the powder at room temperature. A CHPT process (e.g., [24]) utilizes a die to confine its sample. This eliminates the drawbacks of the conventional HPT process such as materials' flash out [25], effect of anvils' misalignment [25, 26] and presence of dead zone [26, 27]. The confinement also reduces the process conditions and enables to fabricate metallic hybrid materials with low to moderate parameters of 1.5 GPa and 2 rotations. Fabrication of metallic composites by CHPT eliminates a need for a subsequent heat treatment and therefore reduces energy consumption [28] during the manufacturing. Owing to the SPC's simplicity, it can also be used as an experimental framework to physically simulate and study similar processes. Different properties of the densified particles such as their post deformation size, morphology, grain refinement, density and shear strength can be easily studied and correlated to the process parameters.

This work aims to demonstrate the SPC process and its merits. It also aims to explain the resulted properties based on scanning electron microscope (SEM) and electron backscatter diffraction (EBSD) maps in the processed materials. The scope of this work includes demonstrating the process, its requirements and its ability to enhance material's mechanical properties and to explore distribution of the properties in the densified zone. To investigate the sample's properties in the consolidated powder region, the micro hardness tests and micro shear punch test (MSPT) are utilized. Also the MSPT's data are interpreted using a dedicated dimensional theory. The SEM and EBSD observations revealed a significant grain refinement in both copper and aluminum regions. The MSPT's, performed on the densified aluminum zone, showed a significant improvement in the mechanical properties. The results indicated that the reduction of both particle and grain sizes in the powder zone were responsible for the resulted high shear strength and sub structure formation was responsible for the significant grain refinement in both materials. This was in agreement with the high strength values, characterized by MSPT, in the processed zone. A strong *mechanical bonding* of the filler particles was achieved at room temperature under a moderate pressure and shear deformation. This together with a "radially homogeneous strength-deformation behavior" indicated promising potentials of the SPC to produce composite metal parts at room temperature.

Experimental procedure

To demonstrate the process, micron size commercial purity (99.7 %) aluminum particles (Al eckagranules® 75 s, average particle size of 28 μm) were processed in an oxygen-free copper annulus using the SPC. This produced highly dense, strong, and ductile cylindrical hybrid samples.

Basics of the SPC are shown schematically in Fig. 1a. The Cu annular was carefully filled with the Al powder before being confined in the die and was held between the upper and lower punches. The pressure and shear were applied to the SPC sample using a servo hydraulic HPT setup followed by rotating the bottom punch to produce friction induced shear deformation in the sample. The morphology of the powder particles and the microstructure of the unprocessed copper are shown in Fig. 1b, c.

Copper rings with 16 mm outer diameter, 4 mm height and 2 mm thickness were machined out of oxygen-free copper C11000 with 99.90 % purity and used in these experiments. Average grain size of copper was 9 μm, without submicron size grains where ~2 % of the grains were ~19 μm in size.

Immediately before filling the copper ring with the Al powder, it was mechanically cleaned using a 2500 grade emery paper to remove the oxide layer, washed with deionized water and dried. The copper annulus was slowly

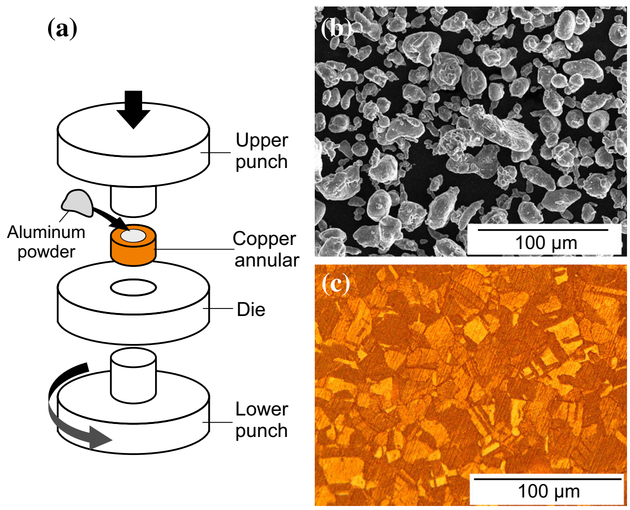

Fig. 1 Experimental setup for SPC **a** schematic diagram of the process **b** morphology of Al powder **c** micro structure of copper as received

filled with the aluminum powder, before processing the filled annulus. More details on the careful considerations undertaken to prevent the material contamination during the preparation and handling stages could be found elsewhere [29].

The prepared composite assembly was processed next to fabricate SPC samples. The process conditions included a combined normal pressure of 1.5 GPa and 2 revolutions at room temperature.

Results and discussion

Overall morphology of the processed sample is shown in Fig. 2a where *concentric circular shearing lines* are visible. Electron Back Scatter Diffraction (EBSD) analyses were conducted on transverse section of the SPC fabricated disks using 20 kV at a working distance of 10 mm with a spot size of 2.5 (11 nA) under analytical mode, using hexagonal grid, 4 × 4 binning, with an exposure time of 5.17 and gain of 7.1 with a step size of 0.05 μm. The crystal orientation maps (COM's) were obtained using FEI Quanta 3D FEG SEM and TSL OIM analysis software. To explore deformation at a grain boundary level for Al and Cu, crystal orientation map (COM) of as received copper (Fig. 2b) and COM's of deformed material were obtained and studied. The maps confirmed formation of fine grains in the parent materials due to the SPC processing; substructures are shown in the aluminum at point 1 near the center region (Fig. 2c), point 2 near the interface region (Fig. 2d) and at point 3 in copper zone near the interface (Fig. 2e). The COM maps also confirmed the formation of

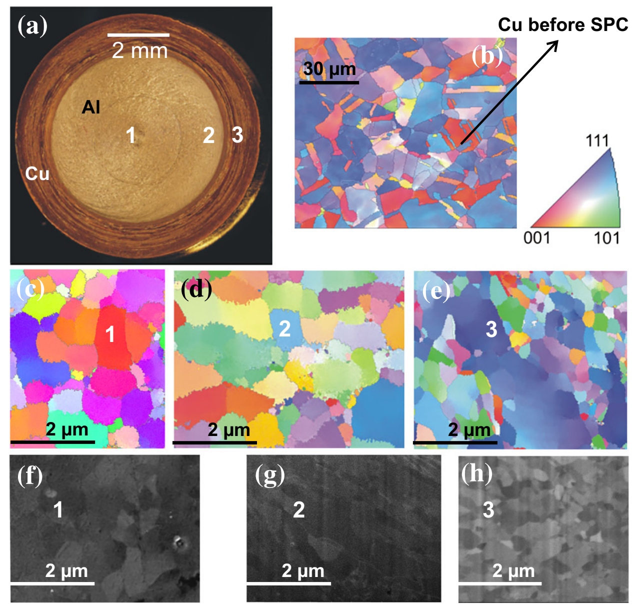

Fig. 2 Morphology and microstructure of the SPC processed sample. **a** Composite sample and positioning of three probing points1, 2, and 3. **b** COM of Cu before SPC. **c–e** COM of Al and Cu zones near points 1, 2, and 3, respectively. **f–h** SEM images of Al and Cu zones near points 1, 2, and 3, respectively

submicron grains (less than 1 μm) in both aluminum and copper after processing.

Scanning electron microscopy (SEM) maps were also developed using the same FEI Quanta 3D FEG SEM at the same regions corresponding to the EBSD analysis. SEM observations also confirmed the submicron size grain refinement and sub structure of the grains in both aluminum and copper. Elongated structure for aluminum near the interface region (point 2 in Fig. 2d, g) can be due to a sticking boundary condition between the parent materials at their interface.

Benchmarking the material's properties in the consolidated powder region

Micro hardness measurements have been commonly used to assess strength of powder compacted parts using HPT [30, 31].

For benchmarking of the SPC sample's strength and its distribution in the Al zone, four *sample types* were used: the SPC samples, SPC samples without torsion (control sample), a commercially pure Al (CP-Al) solid sample and an aluminum alloy Al 5005-H34 solid sample.

We performed micro hardness tests using 10 g load with 15 s dwelling time using a Matsuzawa micro hardness tester MHT-1 according to ASTM: E384 11e1 [32]. In order to avoid the variation in hardness distribution in top and bottom surfaces as described in a HPT process [31], the hardness measurements were taken over mid-plane of the processed sample along three equally spaced radial directions (60° apart, directions 1, 2, and 3) and the results are shown in Fig. 3. An average hardness of ~44 kgf/mm^2 can be seen in Fig. 2 within the aluminum region. The average hardness of CP-Al and Al 5005-H34 samples were also measured to compare with the SPC processed sample. The pure CP-Al sample had an average hardness of 17.7 kgf/mm^2 which is significantly lower than that of the SPC processed sample. Also, the Al 5005-H34 sample had an average hardness of 53.2 kgf/mm^2 which lies between the lowest and the highest limits of the processed material's hardness values shown in Fig. 3. An average hardness of ~61 kgf/mm^2 was also measured for Cu before the process. Hardness results of the copper region after the process (Fig. 3), between 70 and 82 kgf/mm^2, also show an increased hardness. The maximum hardness values are consistently located at the Al-Cu interface which indicates a sticking boundary condition at the interface during the SPC. This is based on an assumption that hardness is directly related to work hardening caused by the SPC. Also, a minimum work hardening at the center is consistent with the typical velocity field used for HPT tests.

A micro hardness measurement, with a small 10 g load, is an indication of the surface strength instead of an overall measure of strength across the specimen's thickness. Care must be taken when interpreting such measurements for the Al zone due to the likely presence of pores in the vicinity of the intender. The measurement is also a point value which represents the surface strength immediately after the SPC. It is desirable to have an understanding of the overall mechanical properties of the sample across its thickness and to evaluate material's response under loading up to its failure. Given the small size of SPC sample, this was achieved in the current work using the micro shear punch test. In order to gather preliminary understanding of the material performance after SPC processing, the tests were performed at different radii of the sample.

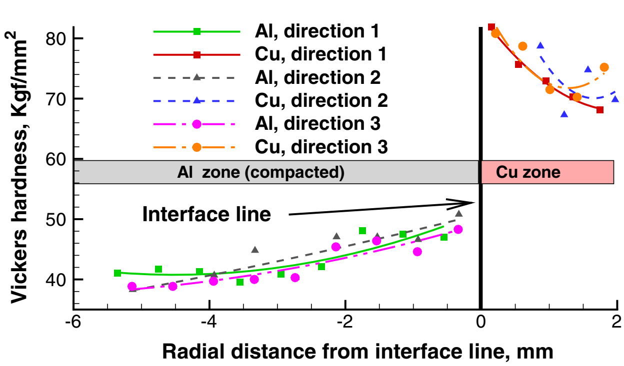

Fig. 3 Vickers hardness at the mid-plane of the MSP sample in Al and Cu zones along its radius with respect to the interface line

Micro shear punch tests and density measurements in the Al zone

Micro shear punch test (MSPT) has been used as a small specimen test technique by several researchers [33]. Given its relatively small punch size, the test enables a preliminary and comparative study of material performance within a small footprint when there is a gradient of properties across the sample.

Figure 4a shows a MSPT setup [34] which was used in this research. The tests were undertaken at four points in Al zone of the SPC samples which were prepared for the MSPT. The preparations included manual grounding of the SPC samples to a thickness of $t = 2$ mm. Each test was performed with a punch radius of $r_p = 1.5$ mm (Fig. 4a). Sliding the prepared sample horizontally prior each test allows punching holes in different locations within the Al zone (different $r_i^\prime s$ in Fig. 4b, $0 \le r_i \le 6$ mm). Figure 4c shows positioning of the four punch holes produced by the MSP at different radii in the Al zone. The control sample fractured during the MSPT (Fig. 4d). This suggests that a minimum pressure and shear should be applied concurrently for an effective particle bonding. Figure 4e compares variation of shearing strength $\tau = F_s/S_p$ versus engineering strain $\varepsilon = z/t$ for the four sampling points and those of the solid CP-Al and Al 5005-E34 samples using the MSPT results where F_s, $S_p = 2\pi r_p t$ and z are the MSPT force, punch's shearing area and punch's penetration depth in the sample, respectively. The MSP test for the Al 5005-H34 sample was carried out at two different point T1 and T2 (Fig. 4e) to confirm material's homogeneity and the repeatability of the test. All of the tests were performed with a strain rate of $\dot{\varepsilon} = 0.01\ s^{-1}$.

The MSPTs' pieces, blanked pieces from the SPC samples shown in Fig. 4b, revealed the typical "fracture" and "burnish" zones around them as an indication of a ductile fracture. The control samples did not produce reliable MSPT data as they had a brittle fracture as shown in Fig. 4d. It is clear that the SPC sample (with a $F_{smax} \cong 740N$) is nearly "four times" stronger than the solid CP-Al sample (Fig. 4e). The peak shearing strengths for both SPC and Al 5005-H34 samples are nearly identical. However, the former reaches its peak much earlier than the latter. This indicates that the SPC's sample is less formable compared to the solid Al samples.

Density ratio distribution along the sample's radius was investigated using the MSPT's blanked pieces. A maximum density ratio of 99.3 % at the Al zone's center was observed which linearly reduced to its minimum of 98.2 % at point 3 in Fig. 4c (the closest of the 4 points to the Al-Cu interface).

MSPT results at different radii locations show nearly similar deformation behavior and are in good agreement

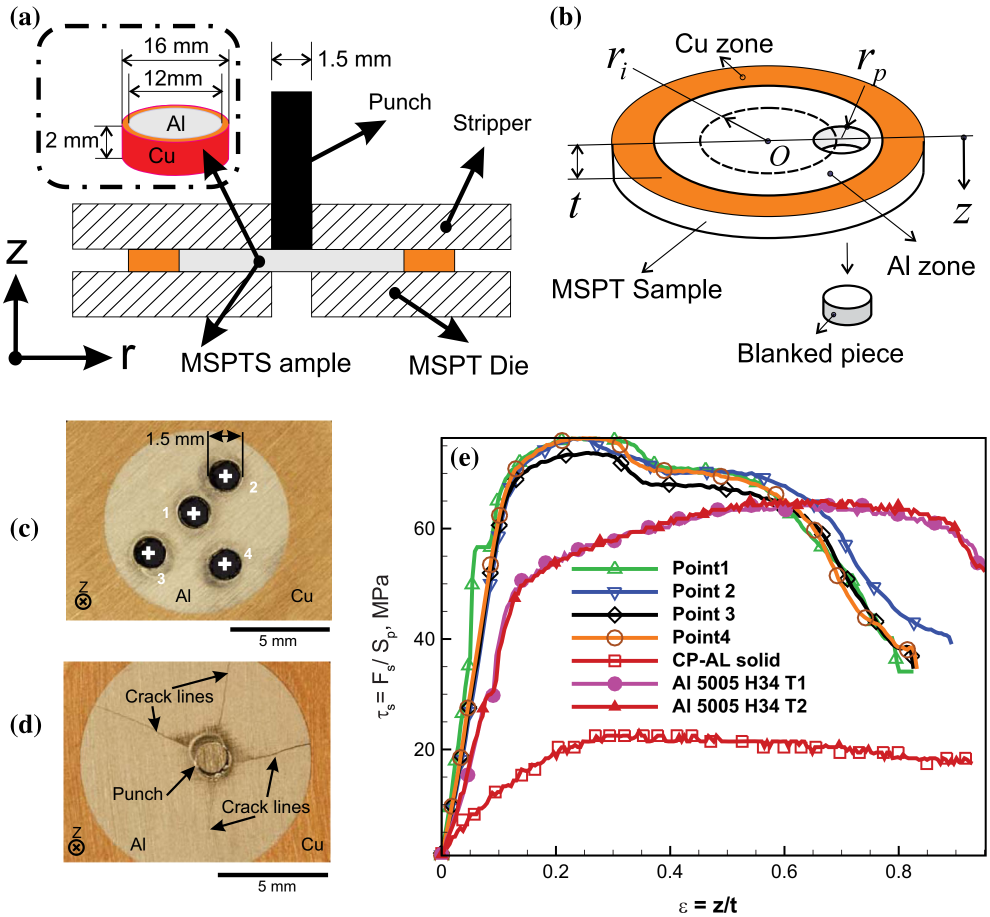

Fig. 4 **a** Schematic of the MSPT, **b** a MSPT sample produced from the SCP product, **c** positioning of the MSPT points, **d** failure of the control sample during MSPT **e** distribution of shearing strength $\tau_s = F_s/S_p$ versus $\varepsilon = z/t$ at the four points and their comparison with that of solid Al MSPT samples

with the micro structures obtained at those sampling points (Fig. 2). Although a small increase in the harness is observed in the radial direction, sample's density ratio slightly reduces in the radial direction which can compromise the radial gradient of hardness. Therefore, based on these observations one could conclude that the solidification of the powder particles in this SPC process has been distributed in a homogeneous fashion.

Bonding strength of aluminum and copper

The current process was undertaken at room temperature. As a result, a physical/geometrical locking are expected at the interface of the two materials. An interfacial examination of the interface was carried out and the result is shown in Fig. 5a. This scanning electron microscopy examination demonstrates a curved profile of the interface. Due to the geometrical complexity of the concave longitudinal interface, shown in Fig. 5a, two rotational and two translational degrees of freedom at the interface are physically constrained. This leaves only two unconstrained degrees of freedom. These include on degree of freedom along the instantaneous normal to the interface plane (translation) and one about the longitudinal axis (torsion), respectively. In the presence of a metallurgical bound at the interface, the two degrees of freedom will be eliminated, thus resulting in a stronger structure. Exploring the nature of bonding at the Al-Cu interface is beyond the scope of current work. Undertaking the process under sufficiently high temperatures can provide metallurgical bonding.

In this section, a "lower limit" estimation of the bonding strength is presented by excluding a possibility of metallurgical bonding at the interface. Given the specific degrees of freedom described here, it is expected that the hybrid/composite sample to demonstrate a directional strength behavior. In a similar study [35] the bonding strength of a hybrid sample was measured using a dedicated blanking test. While this is a convenient way of measuring the bonding strength for a cylindrical interface, it is not practical for the complex interface geometry shown in Fig. 5a. Disintegration of the components in the hybrid sample in the longitudinal sample seems to be the most

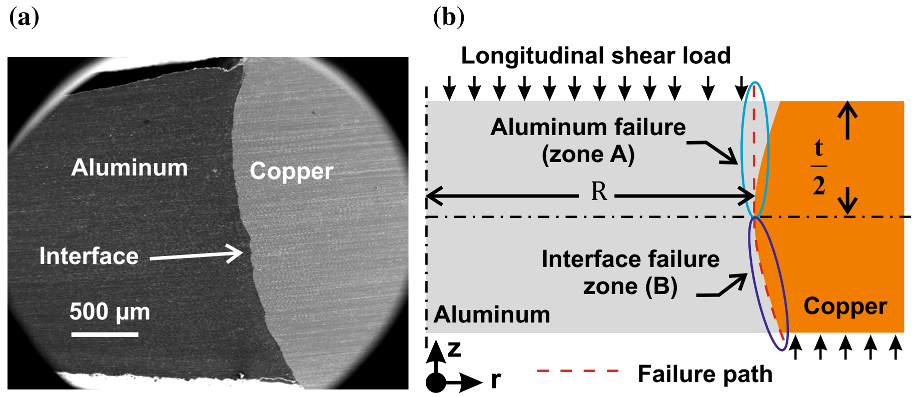

Fig. 5 **a** Back scatter electron (BSE) image obtained for the cross section of the SPC processes sample showing the curved interface and **b** illustration of the potential mechanism during a shear failure of the Cu-Al joint

likely mode of failure. Therefore, an estimation of the sample's bonding strength in the longitudinal direction, based on a "failure path" concept shown in Fig. 5b, is presented here.

Since the MSPT results show a behavior which are reasonably independent of the foot print location, r_i, a nearly uniform shearing strength in the aluminum core can be assumed. In this zone, the shear strength of the aluminum region, τ_s, can be estimated using $\tau_s = F_s/S_p$; where shearing area is $S_p = 2\pi r_p t$.

Figure 5b illustrates a potential failure path of the composite material during a longitudinal shear loading. Initially the softer material (Al in this pair) can act as the crack arrester in a cause of failure as indicated in the zone A. However, due to orientation of the concave interface profile in zone B, a negligible bonding strength may be considered for this part of the sample subjected to the shearing load. Based on the proposed "longitudinal failure path (vertical) in zone A" (Fig. 5b), the zone withstands the shear load in the longitudinal direction. Once the shear action completes in this zone, zone B arrests the crack along its interface. Assuming a non-metallurgical bond between Al-Cu in zone B, the crack propagation in the zone can be considered as simple separation of the two metals requiring a minimum/zero shearing load. Based on the SEM profile of the interface, shown in Fig. 5a, it is assumed that zone A comprises half of the sample's thickness (t/2). These assumptions allow a lower limit estimation of the bonding strength.

Given a sample of t in thickness, a shearing load limit of $F_{\min} = \pi R \tau t$ can be estimated. Therefore, the minimum required force to blank a 2 mm sample and core radius of $R = 6$ mm is estimated as $F_{\min} \cong 2674N$.

A key advantage of SPC is its *moderate* "process requirements". These are easier to achieve in comparison with similar processes such as HPT; typical recommended pressures and number of revolutions for a significant grain refinement in bulk and powdered materials by HPT are between 7 to 25 GPa and 15–60 revolutions, respectively [36–38]. The presented results demonstrate the SPC's ability in fabricating strong metal composite hybrid samples under a much lower pressure and lower number of revolution; a concurrent pressure of up to 1.5 GPa with 2 revolutions. These makes the SPC process even a more attractive solution for effective powder consolidation and grain refinement in hollow parts at room temperature.

Conclusions

A new process, SPC, was introduced to fabricate hybrid metallic composites at room temperature. To demonstrate the potentials of the SPC, composite Cu-Al samples were manufactured and characterized using microstructural-crystallographic maps, micro hardness measurements, the MSPT and compaction density measurements. To produce strong densified powder at room temperature using the SPC, the process requirements were significantly lower than those typically needed for HPT. Moderate concurrent pressure and shear of 1.5 GPa and 2 revolutions, respectively, led to formation of submicron grains in both zones of the hybrid material. The promising grain refinement is in good agreement with a reasonably uniform distribution of shear punch response in the consolidated aluminum region. A potential failure analysis of the curved interface with mechanical interlocking was employed to estimate the lower limit bonding of the aluminum–copper joint in the longitudinal direction. It was found that approximately 2674 N was required to separate the aluminum–copper joint of a 2-mm-thick sample.

The SPC process proved to be an effective technique to make strong hybrid composite metals at room temperature. The homogeneous property improvement under moderate processing conditions is quite significant in terms of energy and material saving. Using powder as the filler in various hollow parts, this room temperature process has good potentials to manufacture metallic composite parts with a strong particle bonding.

Acknowledgements The authors acknowledge the use of the facilities and assistance of Dr. Amelia Liu and Dr. Annalena Wolff at the Monash Centre for Electron Microscopy and the support received from Monash University Postgraduate Publication Award scheme.

References

1. Ibrahim IA, Mohamed FA, Lavernia EJ (1991) Particulate reinforced metal matrix composites—a review. J Mater Sci 26:1137–1156. doi:10.1007/BF00544448
2. Nawa M, Sekino T, Niihara K (1994) Fabrication and mechanical behaviour of Al_2O_3/Mo nanocomposites. J Mater Sci 29:3185–3192. doi:10.1007/BF00356661
3. Bouaziz O, Kim HS, Estrin Y (2013) Architecturing of metal-based composites with concurrent nanostructuring: a new paradigm of materials design. Adv Eng Mater 15:336–340
4. Embury D, Bouaziz O (2010) Steel-based composites: driving forces and classifications. Annu Rev Mater Res 40:213–241
5. Bouaziz O, Bréchet Y, Embury JD (2008) Heterogeneous and architectured materials: a possible strategy for design of structural materials. Adv Eng Mater 10:24–36
6. Beygelzimer Y, Reshetov A, Synkov S, Prokof'eva O, Kulagin R (2009) Kinematics of metal flow during twist extrusion investigated with a new experimental method. J Mater Process Technol 209:3650–3656
7. Shamdani AH, Khoddam S, Thomson PF, Dehghan-Manshadi A (2012) Microstructure and mechanical properties of IF steel deformed during plane stress local torsion. J Mater Sci 47:1582–1587. doi:10.1007/s10853-011-6121-4
8. Lapovok R, Ng HP, Tomus D, Estrin Y (2012) Bimetallic copper–aluminium tube by severe plastic deformation. Scripta Mater 66:1081–1084
9. Zebardast M, Taheri AK (2011) The cold welding of copper to aluminum using equal channel angular extrusion (ECAE) process. J Mater Process Technol 211:1034–1043
10. Sapanathan T, Khoddam S, Zahiri SH, Zarei-Hanzaki A (2014) Strength changes and bonded interface investigations in a spiral extruded aluminum/copper composite. Mater Des 57:306–314
11. Sapanathan T, Khoddam S, Zahiri SH (2013) Spiral extrusion of aluminum/copper composite for future manufacturing of hybrid rods: a study of bond strength and interfacial characteristics. J Alloy Compd 571:85–92
12. Zhilyaev AP, Langdon TG (2008) Using high-pressure torsion for metal processing: fundamentals and applications. Prog Mater Sci 53:893–979
13. Estrin Y, Janecek M, Raab GI, Valiev RZ, Zi A (2007) Severe plastic deformation as a means of producing ultra-fine-grained net-shaped micro electro-mechanical systems parts. Metall Mater Trans A 38:1906–1909
14. Zhu YT, Lowe TC, Langdon TG (2004) Performance and applications of nanostructured materials produced by severe plastic deformation. Scripta Mater 51:825–830
15. Yang NYC, Headley TJ, Kelly JJ, Hruby JM (2004) Metallurgy of high strength Ni–Mn microsystems fabricated by electrodeposition. Scripta Mater 51:761–766
16. Bachmaier A, Pippan R (2011) Effect of oxide particles on the stabilization and final microstructure in aluminium. Mater Sci Eng, A 528:7589–7595
17. Tokunaga T, Kaneko K, Sato K, Horita Z (2008) Microstructure and mechanical properties of aluminum–fullerene composite fabricated by high pressure torsion. Scripta Mater 58:735–738
18. Kaneko K, Hata T, Tokunaga T, Horita Z (2009) Fabrication and characterization of supersaturated al-mg alloys by severe plastic deformation and their mechanical properties. Mater Trans 50:76–81
19. Botta Filho W, Fogagnolo J, Rodrigues C, Kiminami C, Bolfarini C, Yavari A (2004) Consolidation of partially amorphous aluminium-alloy powders by severe plastic deformation. Mater Sci Eng A 375:936–941
20. Yavari AR, Botta Filho W, Rodrigues C, Cardoso C, Valiev R (2002) Nanostructured bulk Al 90 Fe 5 Nd 5 prepared by cold consolidation of gas atomised powder using severe plastic deformation. Scripta Mater 46:711–716
21. Lee Z, Zhou F, Valiev R, Lavernia E, Nutt S (2004) Microstructure and microhardness of cryomilled bulk nanocrystalline Al–7.5% Mg alloy consolidated by high pressure torsion. Scripta Mater 51:209–214
22. Beygelzimer Y, Estrin Y, Kulagin R (2015) Synthesis of hybrid materials by severe plastic deformation: a new paradigm of SPD processing. Adv Eng Mater 17:1853–1861
23. Khoddam S, Estrin Y, Kim HS, Bouaziz O (2015) Torsional and compressive behaviours of a hybrid material: spiral fibre reinforced metal matrix composite. Mater Des 85:404–411
24. Khoddam S, Sapanathan T, Zahiri S, Hodgson PD, Zarei-Hanzaki A, Ibrahim R (2015) Inner architecture of bonded splats under combined high pressure and shear. Adv Eng Mater. doi:10.1002/adem.201500418
25. Huang Y, Kawasaki M, Langdon TG (2013) Influence of anvil alignment on shearing patterns in high-pressure torsion. Adv Eng Mater 15:747–755
26. Hohenwarter A, Bachmaier A, Gludovatz B, Scheriau S, Pippan R (2009) Technical parameters affecting grain refinement by high pressure torsion. Int J Mater Res 100:1653–1661
27. Lee DJ, Yoon EY, Park LJ, Kim HS (2012) The dead metal zone in high-pressure torsion. Scripta Mater 67:384–387
28. Rekha M, Laishram K, Gupta RK, Malhan N, Satsangi AK (2009) Energy-efficient green synthesis of Nd:Y_2O_3 nanopowder by microwave gel combustion. J Mater Sci 44:4252–4257. doi:10.1007/s10853-009-3615-4
29. Sapanathan T (2015) Fabrication of axi-symmetric hybrid materials using combination of shear and pressure. PhD Thesis (Doctorate), Faculty of Engineering, Department of Mechanical and Aerospace Engineering, Monash University, Melbourne
30. Asgharzadeh H, Joo SH, Kim HS (2014) Consolidation of carbon nanotube reinforced aluminum matrix composites by high-pressure torsion. Metall Mater Trans A 45:4129–4137
31. Cubero-Sesin JM, Horita Z (2012) Powder consolidation of Al–10wt% Fe alloy by high-pressure torsion. Mater Sci Eng A 558:462–471
32. ASTM E384-11e1 (2011) Standard test method for Knoop and Vickers hardness of materials. ASTM International, West Conshohocken, PA
33. Sokolov MA, Landes JD, Lucas GE (2002) Small specimen test techniques, vol 4. ASTM International, West Conshohocken, PA
34. Farhoumand A, Khoddam S, Hodgson PD (2012) A study of plastic deformation during axisymmetric forward spiral extrusion and its subsequent mechanical property changes. Modell Simul Mater Sci Eng 20(8):1–15
35. Sapanathan T, Ibrahim R, Khoddam S, Zahiri SH (2015) Shear blanking test of a mechanically bonded aluminum/copper composite using experimental and numerical methods. Mater Sci Eng A 623:153–164
36. Zrnik J, Pippan R, Scheriau S, Kraus L, Fujda M (2010) Microstructure and mechanical properties of UFG medium carbon steel processed by HPT at increased temperature. J Mater Sci 45:4822–4826. doi:10.1007/s10853-010-4482-8
37. Zhilyaev AP, McNelley TR, Langdon TG (2007) Evolution of microstructure and microtexture in fcc metals during high-pressure torsion. J Mater Sci 42:1517–1528. doi:10.1007/s10853-006-0628-0
38. Patil DC, Kori SA, Venkateswarlu K, Das G, Alhajeri SN, Langdon TG (2013) Using ball indentation to determine the mechanical properties of an Al-7475 alloy processed by high-pressure torsion. J Mater Sci 48:4773–4779. doi:10.1007/s10853-012-6969-y